

# Optimal Control for Electron Shuttling

Jun Zhang<sup>1,2</sup>, Loren Greenman<sup>2</sup>, Xiaotian Deng<sup>2</sup>, Ian M. Hayes<sup>2</sup>, and K. Birgitta Whaley<sup>2</sup>

<sup>1</sup>*Joint Institute of UM-SJTU, Shanghai Jiao Tong University,  
and Key Laboratory of System Control and Information Processing,  
Ministry of Education, Shanghai, 200240, China*

<sup>2</sup>*Department of Chemistry, Berkeley Center for Quantum Information and Computation,  
University of California, Berkeley, California 94720, USA*

(Dated: October 16, 2018)

In this paper we apply an optimal control technique to derive control fields that transfer an electron between ends of a chain of donors or quantum dots. We formulate the transfer as an optimal steering problem, and then derive the dynamics of the optimal control. A numerical algorithm is developed to effectively generate control pulses. We apply this technique to transfer an electron between sites of a triple quantum dot and an ionized chain of phosphorus dopants in silicon. Using the optimal pulses for the spatial shuttling of phosphorus dopants, we then add hyperfine interactions to the Hamiltonian and show that a 500 G magnetic field will transfer the electron spatially as well as transferring the spin components of two of the four hyperfine states of the electron-nuclear spin pair.

## I. INTRODUCTION

The benefits of implementing a quantum computer in silicon [1], namely the ability to exploit the techniques of the semiconductor industry and long electron and nuclear spin coherence times, has been offset with challenges including the coupling of qubits. One mechanism for exchanging quantum information between qubits is electron shuttling, in which spin or charge qubits are physically moved between local sites [2]. For dopant spin qubits in silicon [3], electron shuttling has been proposed using voltage gates and pulses designed analogously to the Stimulated Raman Adiabatic Passage (STIRAP) procedure [4]; this procedure is referred to as Coherent Tunneling by Adiabatic Passage (CTAP) [5–7]. Similar mechanisms have been suggested [7, 8] for quantum dots, which have also been proposed as qubits [9, 10] in silicon [11–13] as well as other materials such as GaAs [14, 15]. CTAP and other adiabatic procedures avoid populating undesired sites at any point during the transfer, thereby eliminating issues of decoherence associated with a specific site. However, if the source of decoherence is not site-specific or is controllable by alternative means, it may be useful to approach the state transfer problem for silicon qubits using optimal control theory instead. Optimal controls which minimize transfer time or (as will be explored here) minimize pulse fluence have been shown to minimize decoherence due to additive and multiplicative white noise, respectively [16, 17]. Such noise sources can arise from thermal fluctuations of carriers. Another noise source can arise from variations in the devices due to the manufacturing, this introduces  $1/f$  noise, and it will be seen that our fluence-minimized pulses are dominated by high-frequency components. Additionally, for qubits such as charge qubits in which site-specific decoherence is not the main problem, we can use optimal controls to minimize the energy required for gate operations.

In this paper we will investigate the shuttling of electrons between the ends of a qubit chain using optimal

control theory. Depending on whether the chain represents dopant spin qubits [5, 7] or lateral quantum dots [8], the control fields will affect the tunnel couplings between dopants or the on-site energy of a quantum dot, respectively. The task is to design some appropriate control fields to transport the electron to the end of the qubit chain. During this process, quantum information can be passed through along the array so as to realize the desired quantum information processing in the solid-state quantum bits.

We have formulated this problem as an optimal steering problem in control theory in a state space of all of the density matrices. The system dynamics is governed by the Liouville-von Neumann equation,

$$i\dot{\rho} = [H, \rho]. \quad (1)$$

We use density matrices to formulate the steering problem in order to make the extension to open systems clear. The Hamiltonian contains several control terms that can be altered externally to guide the system towards a desired result, as well as a fixed drift term that is determined by the physical nature of the system. The objective of steering is to find control fields that transfer the system from an initial state to a final state at a finite terminal time. This is also known as the *constructive controllability* problem [18].

One way to solve the constructive controllability problem is to impose a cost function, which may steer towards a minimum pulse energy, a shortest transfer time, or a minimum error sum over all time steps. We can then employ standard optimal control techniques such as the Pontryagin maximum principle [19] to derive optimality conditions for the control fields.

In the current paper we derive the underlying dynamics that govern the time evolution of the optimal control pulses that minimize the pulse fluence. We choose this cost function partially for mathematical reasons, namely that it provides a numerically well-behaved set of equations for this and other numerical algorithms including

the Krotov method [20–23], but also because this choice of cost function minimizes heating in the devices which would lead to decoherence as well as to effects of multiplicative white noise. We take an intuitive approach, which yields the same results as a more formal approach using the Lie-Poisson reduction theorem [24]. For a given initial condition, the resulting dynamics completely determine the time evolution trajectories of the control pulse. Hence, to solve for control fields that achieve the desired state transfer, we just need to find an appropriate initial condition. Finding such initial conditions thus becomes an optimization problem on real finite-dimensional space.

To solve the Liouville-von Neumann equation (1) numerically, we divide the total time into a number of steps and then use piecewise constant functions to approximate time-varying control fields. The fidelity of the achieved state,

$$F = \text{Tr } \rho_T \rho(T), \quad (2)$$

with  $\rho_T$  representing the desired state, thus depends on all of the piecewise constant control values, which themselves are dependent on the initial conditions of the dynamics as discussed above. Using the chain rule, we can obtain the gradient of the fidelity with respect to the initial condition in an explicit form. With this approach we can implement gradient algorithms to solve for the initial conditions that lead to the optimal control fields.

To exemplify this approach, we investigate here the electron shuttling problem for three-donor systems. Our control algorithm derivation can be readily extended to systems with more donors. We demonstrate the efficacy of our control algorithm by applying it to two physical systems taken from Refs. [5] and [8], namely electron shuttling across a chain of quantum dots and across a chain of phosphorus donors implanted in silicon.

## II. MATHEMATICAL BACKGROUND AND FORMULATION

In this section we summarize the mathematical representation of the electron shuttling problem and introduce some necessary mathematical background for an optimal control treatment of this.

We consider here physical devices in which the spatial location of the electron may be represented by three qubits [5, 7, 8]. The physical systems of interest in this work describe the shuttling of a single electron between either three quantum dots or three donor ions. In both cases, the electron is moving between distinct spatial locations or “sites”. Formally, the presence or absence of the electron on a given site is then represented by the state of a qubit indexed by that site. For shuttling across a chain of quantum dots, the qubit state coding for presence of an electron corresponds to the state of the electron in a discrete energy level of the quantum dot. For shuttling across a chain of phosphorus donors implanted

in silicon, the qubit state coding for presence of an electron corresponds to a neutral donor atom, *i.e.*, the electron is bound to the phosphorus nucleus at that site. Within these simplified physical representations of electron shuttling over three sites, the system Hamiltonian is defined on the Lie algebra  $\mathfrak{su}(3)$ , *i.e.*, all  $3 \times 3$  skew-Hermitian matrices. The dynamics of the electron are determined by the Liouville-von Neumann equation (1), with  $\rho \in \mathbb{C}^{3 \times 3}$  as the density matrix of the three-site system. Note that the density matrix is a Hermitian matrix with unit trace. The Hamiltonian  $H$  can be written in a general form as (setting  $\hbar = 1$ )

$$iH = iH_0 + \sum_{l=1}^8 u_l X_l = \sum_{l=1}^8 a_l X_l + \sum_{l=1}^8 u_l X_l, \quad (3)$$

where  $H_0$  is the drift term,  $u_l$  are control fields, and the matrices  $X_i$  define a basis for  $\mathfrak{su}(3)$ ,

$$\begin{aligned} X_1 &= \begin{bmatrix} 0 & i & 0 \\ i & 0 & 0 \\ 0 & 0 & 0 \end{bmatrix}, & X_2 &= \begin{bmatrix} 0 & 0 & 0 \\ 0 & 0 & i \\ 0 & i & 0 \end{bmatrix}, \\ X_3 &= \begin{bmatrix} 0 & 0 & 1 \\ 0 & 0 & 0 \\ -1 & 0 & 0 \end{bmatrix}, & X_4 &= \begin{bmatrix} 0 & 1 & 0 \\ -1 & 0 & 0 \\ 0 & 0 & 0 \end{bmatrix}, \\ X_5 &= \begin{bmatrix} 0 & 0 & 0 \\ 0 & 0 & 1 \\ 0 & -1 & 0 \end{bmatrix}, & X_6 &= \begin{bmatrix} 0 & 0 & i \\ 0 & 0 & 0 \\ i & 0 & 0 \end{bmatrix}, \\ X_7 &= \begin{bmatrix} i & 0 & 0 \\ 0 & -i & 0 \\ 0 & 0 & 0 \end{bmatrix}, & X_8 &= \frac{1}{\sqrt{3}} \begin{bmatrix} i & 0 & 0 \\ 0 & i & 0 \\ 0 & 0 & -2i \end{bmatrix}. \end{aligned} \quad (4)$$

Note that this basis is just a rearrangement of the Gell-Mann matrices [25]. The density matrix equation of motion is then determined by the Liouville-von Neumann equation (1) with the Hamiltonian given in (3).

The desired high fidelity implementation of electron shuttling amounts to designing control functions  $u_l$  that transfer the density matrix  $\rho$  from the initial state

$$\rho_0 = \begin{bmatrix} 1 & 0 & 0 \\ 0 & 0 & 0 \\ 0 & 0 & 0 \end{bmatrix} \quad (5)$$

at time  $t = 0$  to the final state

$$\rho_T = \begin{bmatrix} 0 & 0 & 0 \\ 0 & 0 & 0 \\ 0 & 0 & 1 \end{bmatrix} \quad (6)$$

at time  $t = T$ .

## III. OPTIMAL CONTROL FORMULATION AND NUMERICAL ALGORITHM

To solve the state transfer problem presented in Eqs. (1), (3), (5), and (6), we formulate an optimal control problem by imposing a cost function, and then use

Pontryagin's maximum principle [19] to derive the optimality conditions. Based on these conditions, we can develop an effective numerical algorithm to solve for the values of the control fields.

### A. Optimal control formulation

In a typical control problem, we apply external control fields to a system with the expectation that it will evolve towards a desired state or objective. The transfer of a system from an initial state to a desired final state is often referred to as the *controllability* problem. The criteria to determine controllability for a general nonlinear system were studied in Refs. [26, 27], and the extensions to quantum mechanical systems were reported in Refs. [28, 29].

From the controllability analysis for control systems on Lie groups, it can be concluded that the system is controllable provided that the drift term  $H_0$  and control terms  $X_l$  in Eq. (3) can generate the Lie algebra  $\mathfrak{su}(3)$  [18, 30]. However, such an analysis gives us only an existence result; it does not tell us how to generate the necessary control fields. What we are more interested is the constructive controllability, *i.e.*, finding the controls that realize the state transfer.

One method of solving this problem is to impose a cost function to the state transfer problem and then apply an optimal control method such as the Pontryagin maximum principle [19]. This yields a set of differential equations which must be satisfied by the control fields. In the following section, we illustrate the construction of these equations for the electron shuttling problem.

We seek the control fields that not only realize the desired state transfer but also minimize the cost function, where the latter is defined as the time integral of a running cost that depends on the control fields  $u$  (from now on, we use  $u$  to denote the finite set of control fields  $u_l$ ):

$$\int_0^T L(u) dt. \quad (7)$$

The integrand  $L$  in Eq. (7), referred to as the *running cost*, can be chosen quite generally to suit different control objectives. For example, when  $L = 1$ , minimization of the cost function will correspond to minimum time control. Here we choose  $L$  as a quadratic function of  $u$ , which allows minimization of pulse fluence:

$$L(u) = \sum_l u_l^2. \quad (8)$$

This choice of cost function minimizes heating in the devices, which can cause decoherence if left unchecked and has also been shown to minimize errors due to multiplicative white noise [16, 31]. With time variable control fields  $u_l(t)$ , the cost function is thus a functional of  $u$ . The optimal control fields are defined as those fields that minimize the cost functional, Eq. (7). The task of finding

the optimal control fields is then expressed mathematically as the task of minimizing the cost functional with respect to all possible variations in all  $u_l(t)$ , *i.e.*, the optimal  $u$  yields

$$\min_{u(\cdot)} \int_0^T L(u) dt. \quad (9)$$

We note that the major motivation to add a cost function at this point is to apply optimal control theory to solve the constructive controllability problem presented in the previous section. For a control Hamiltonian that depends linearly on an unbounded control function, optimal control theory may not be applicable to minimum time control. This is avoided when the running cost  $L$  is chosen to be a quadratic function of the control fields  $u$ , which provides another motivation for the current choice of  $L(u)$ .

There are several possible approaches to solve the resulting optimal control problem. One common method for obtaining numerical solutions to optimal control for quantum systems is the Lagrangian formalism in which a Lagrange multiplier is defined to allow the system dynamics, Eq. (1), to be combined with the cost function to create a new cost functional which is then optimized by solving the associated Euler-Lagrange critical equations [32–34]. We employ here the alternative Hamiltonian approach based on the Pontryagin maximum principle. While for many physical systems of interest the two approaches arrive at equivalent formulations of the equations to be solved for the optimal solutions, these are generally in the form of two point boundary value problems. Numerical solution of such problems often require significant computational power and considerable efforts have been made to develop effective algorithms for their solution [20–23, 35–37]. In the present case however, the Hamiltonian approach of the Pontryagin maximum principle allows for a novel formulation of the optimization as an initial value problem on a finite dimensional space defined by a number of momentum functions [24]. This allows the optimal solutions to be obtained with a relatively straightforward numerical algorithm.

In the Pontryagin approach [38] we define a co-state matrix  $\Psi$  that plays the role of a conjugate variable to  $\rho$  in a (classical) control Hamiltonian

$$\begin{aligned} \mathcal{H} &= \langle \Psi, [-iH, \rho] \rangle + L(u) \\ &= - \left\langle \Psi, \left[ \sum_{l=1}^8 a_l X_l + \sum_{l=1}^8 u_l X_l, \rho \right] \right\rangle + L(u), \end{aligned} \quad (10)$$

where  $\langle X, Y \rangle$  denotes the matrix inner product of  $X$  and  $Y$ :

$$\langle X, Y \rangle = \text{Tr}(XY^\dagger). \quad (11)$$

The equations of motion for  $\Psi$  and  $\rho$  are then obtained

from the Hamilton equations for  $\mathcal{H}$ :

$$\begin{aligned}\dot{\Psi} &= -\frac{\partial \mathcal{H}}{\partial \rho} = -[iH, \Psi] \\ \dot{\rho} &= \frac{\partial \mathcal{H}}{\partial \Psi} = -[iH, \rho].\end{aligned}\quad (12)$$

From this it is evident that the co-state matrix  $\Psi$  plays the formal role of a momentum variable. We distinguish this from the momentum functions defined as [24]

$$\phi_l = \langle \Psi, [X_l, \rho] \rangle. \quad (13)$$

Dimensional analysis shows that in this case the momentum function corresponds formally to a kinetic energy function determined by  $\rho$  and its conjugate variable  $\Psi$ . Substituting these functions in Eq. (10) allows the effective control Hamiltonian to now be written in a compact form

$$\mathcal{H} = -\sum_{l=1}^8 a_l \phi_l - \sum_{l=1}^8 u_l \phi_l + L(u). \quad (14)$$

The optimality condition

$$\frac{d\mathcal{H}}{du} = 0 \quad (15)$$

leads to the following equivalent optimal equations

$$\frac{dL}{du_l} = \phi_l, \quad (16)$$

with  $l = 1, \dots, p$ . This is a set of algebraic equations that can be solved to obtain the optimal controls  $u_l$  as functions of the momentum functions  $\phi_l$ . The complete set of optimality conditions are then as follows:

$$\begin{aligned}\dot{\rho} &= -[iH, \rho], \\ \dot{\Psi} &= -[iH, \Psi], \\ \rho_0 &= \begin{bmatrix} 1 & 0 & 0 \\ 0 & 0 & 0 \\ 0 & 0 & 0 \end{bmatrix}, \quad \rho_T = \begin{bmatrix} 0 & 0 & 0 \\ 0 & 0 & 0 \\ 0 & 0 & 1 \end{bmatrix}, \\ \frac{dL}{du_l} &= \phi_l.\end{aligned}\quad (17)$$

At this point we have arrived at the usual formulation of the optimality conditions as a two-point boundary-value problem. As noted above, in the present situation the numerical challenges associated with solving this may be avoided by transforming the optimization problem to an initial value problem for the momentum functions  $\phi_l$ . We proceed by first obtaining the time derivative of  $\phi_l$ :

$$\begin{aligned}\dot{\phi}_l &= \langle \dot{\Psi}, [X_l, \rho] \rangle + \langle \Psi, [X_l, \dot{\rho}] \rangle \\ &= \langle [-iH, \Psi], [X_l, \rho] \rangle + \langle \Psi, [X_l, [-iH, \rho]] \rangle \\ &= \langle \Psi, [iH, [X_l, \rho]] \rangle - \langle \Psi, [X_l, [iH, \rho]] \rangle \\ &= \langle \Psi, [[iH, X_l], \rho] \rangle,\end{aligned}\quad (18)$$

where the last equality follows from the Jacobi identity [18]. For the Hamiltonian given by Eq. (3) we thereby obtain the following time evolution equation for the momentum functions,

$$\begin{aligned}\dot{\phi}_l &= \left\langle \Psi, \left[ \left[ \sum_{j=1}^8 a_j X_j + \sum_{j=1}^8 u_j X_j, X_l \right], \rho \right] \right\rangle \\ &= \sum_{i=1}^8 \left( \sum_{j=1}^8 a_j C_{jl}^i + \sum_{j=1}^8 u_j C_{jl}^i \right) \phi_i,\end{aligned}\quad (19)$$

where we have introduced the structure constants

$$[X_i, X_j] = \sum_{k=1}^8 C_{ij}^k X_k. \quad (20)$$

Note that the structure constants are antisymmetric in all the indices, *i.e.*,

$$C_{ij}^k = -C_{ji}^k = -C_{kj}^i = -C_{ik}^j, \quad (21)$$

for all  $i, j, k \in \{1, \dots, 8\}$ . Up to antisymmetry, the nonzero structure constants are

$$\begin{aligned}C_{12}^3 &= -1, & C_{14}^7 &= -2, & C_{15}^6 &= 1, \\ C_{24}^6 &= -1, & C_{25}^7 &= 1, & C_{25}^8 &= -\sqrt{3}, \\ C_{34}^5 &= 1, & C_{36}^7 &= 1, & C_{36}^8 &= \sqrt{3}.\end{aligned}\quad (22)$$

Eq. (19) constitutes a set of first order differential equations that govern the dynamical evolution of the momentum functions  $\phi_l$ . When the running cost  $L(u)$  in Eq. (7) is chosen as a quadratic function of the control fields  $u$  (as in Eq. (8)), these functions  $\phi_l$  are linear combinations of the optimal control fields  $u_l$ . It is then straightforward to extract the dynamics of the optimal controls  $u$ . The control problem has thereby been reduced to finding an appropriate initial condition for Eq. (19), a considerably easier task than solving the two-point boundary value problem of Eq. (17).

We note that the functions  $\phi_l$  describe the reduced dynamics from the Lie-Poisson Reduction Theorem [24], and Eq. (19) can also be derived directly from that Theorem. See Chap. 13 of Ref. [24] and Ref. [39] for details.

One useful property of  $\phi$  is that its norm is a conserved quantity along the optimal trajectory. This may be shown by recalling that the structure constants  $C_{jl}^i$  are antisymmetric in all the indices, from which we obtain that

$$\begin{aligned}\frac{d}{dt} \|\phi\|^2 &= \frac{d}{dt} \left( \sum_{l=1}^8 \phi_l^2 \right) = \sum_{l=1}^8 2\phi_l \dot{\phi}_l \\ &= 2 \sum_{l=1}^8 \sum_{i=1}^8 \phi_l \left( \sum_{j=1}^8 a_j C_{jl}^i + \sum_{j=1}^8 u_j C_{jl}^i \right) \phi_i = 0.\end{aligned}$$

Hence,

$$\|\phi\|^2 = \text{const.} \quad (23)$$

## B. Numerical algorithm

We develop a gradient algorithm to find the initial conditions that optimize the fidelity of the final state.

Consider a given time interval  $[0, T]$ . Divide it into  $N$  equal intervals  $\{[t_k, t_{k+1}]\}_{k=0}^{N-1}$  of length  $\Delta t = t_{k+1} - t_k = T/N$ , where  $t_0 = 0$  and  $t_N = T$ . Note that we must choose  $N$  large enough that the evolution equations for the momentum functions (19) are satisfied. Within the interval  $[t_k, t_{k+1}]$ , assume the control fields  $u_l(t)$  takes a constant value  $u_l(k)$  at  $t = t_k$ . Define the fidelity of the actually achieved terminal state  $\rho(T)$  as in Eq. (2). The state transfer problem amounts to maximizing the fidelity  $F$  by finding the optimal control pulses  $u_l(k)$ .

From Eq. (16), we know that the control fields  $u_l(k)$  are determined once the momentum functions  $\phi_l(k)$  are known. Furthermore, the  $\phi_l(k)$  are obtained by solving Eq. (19) with the initial condition  $\phi(0)$  (the vector with components  $\phi_l(0)$ ). Therefore, to maximize the fidelity, we just need to find an appropriate vector  $\phi(0)$ . The advantage of optimizing over  $\phi(0)$  instead of over  $u_l$  is that  $\phi(0)$  is a vector with dimension 8, whereas  $u_l$  has dimension  $N$ , which is usually a much larger number.

The gradient of the fidelity  $F$  with respect to  $\phi_l(0)$ ,  $dF/d\phi_l(0)$ , can be derived explicitly: details are presented in Appendix A. With this gradient in hand we can then formulate a gradient algorithm to determine the optimal initial condition  $\phi^*(0)$ . The other components of this gradient algorithm are solution of the coupled first order equations, Eq. (19) to obtain  $\phi(t)$  and solution of Eq. (16) to obtain the physical control fields  $u_l(t)$  from the  $\phi(t)$ . The full algorithm is then constructed as follows.

### Algorithm 1

1. Choose an initial guess for  $\phi^0(0)$ ;
2. At the  $j$ -th step, solve the differential equation Eq. (19) with the initial condition  $\phi^j(0)$  to get  $\phi_l(k)$ ;
3. Solve the algebraic equation Eq. (16) to get the optimal controls  $u_l(k)$  as functions of  $\phi_l(k)$ ;
4. Follow the procedure in Appendix A to derive  $\nabla_{\phi^j(0)} F$ ;
5. Let  $\phi^{j+1}(0) = \phi^j(0) + \epsilon \nabla_{\phi^j(0)} F$ , where  $\epsilon$  is a small positive number;
6. Repeat Steps (2)–(5) until a desired fidelity is reached.

Note that Khaneja *et al* [40] developed the gradient ascent pulse engineering (GRAPE) algorithm to solve a similar problem. The difference between GRAPE and our algorithm is that GRAPE solves for the control pulses directly, whereas our algorithm optimizes over the initial condition of a differential equation.

We will apply our algorithm to two physical systems, the triple quantum dot system discussed in Ref. [8] and the ionized donor chain discussed in Ref. [5]. For the ionized donor chain we further show that the optimized control fields can also provide a high degree of spin state transfer when the shuttled electron is coupled to the donor nuclei by the hyperfine interaction.

## IV. TRIPLE QUANTUM DOT

We now investigate electron shuttling for the triple quantum dot system discussed in Ref. [8]. In this system, an electron beginning in the left dot of a three lateral quantum dot system is moved to the right dot. The relative energies of the left and right dots are controlled by external gate voltages. The Hamiltonian is given by

$$H = \begin{bmatrix} \mu_L(t) & J_1 & 0 \\ J_1 & 0 & J_2 \\ 0 & J_2 & \mu_R(t) \end{bmatrix}, \quad (24)$$

where the control fields are the on-site energies  $\mu_L$  and  $\mu_R$ , and  $J_1$  and  $J_2$  are the fixed coupling constants between nearest neighboring dots. Using the basis in Eq. (4), we can rewrite the Hamiltonian (24) as

$$iH = J_1 X_1 + J_2 X_2 + \frac{\mu_L}{2} X_7 + \frac{\mu_L - 2\mu_R}{2\sqrt{3}} X_8 + \frac{\mu_L + \mu_R}{3} iI_3 \quad (25)$$

We consider the minimum energy cost function (see Sec. III A):

$$\min \frac{1}{2} \int_0^T (\mu_L^2(\tau) + \mu_R^2(\tau)) d\tau.$$

The parameters in the Hamiltonian of Eq. (3) are

$$a_1 = J_1, \quad a_2 = J_2, \quad u_7 = \frac{\mu_L}{2}, \quad u_8 = \frac{\mu_L - 2\mu_R}{2\sqrt{3}}.$$

Hence

$$\mu_L = 2u_7, \quad \mu_R = u_7 - \sqrt{3}u_8,$$

and the running cost is

$$L(u) = \frac{\mu_L^2}{2} + \frac{\mu_R^2}{2} = 2u_7^2 + \frac{(u_7 - \sqrt{3}u_8)^2}{2}.$$

The optimality condition (16) becomes

$$\phi_7 = 5u_7 - \sqrt{3}u_8, \quad \phi_8 = 3u_8 - \sqrt{3}u_7,$$

which yields

$$u_7 = \frac{\sqrt{3}\phi_7 + \phi_8}{4\sqrt{3}}, \quad u_8 = \frac{\sqrt{3}\phi_7 + 5\phi_8}{12},$$

and hence

$$\mu_L = \frac{\sqrt{3}\phi_7 + \phi_8}{2\sqrt{3}}, \quad \mu_R = -\frac{\phi_8}{\sqrt{3}}.$$

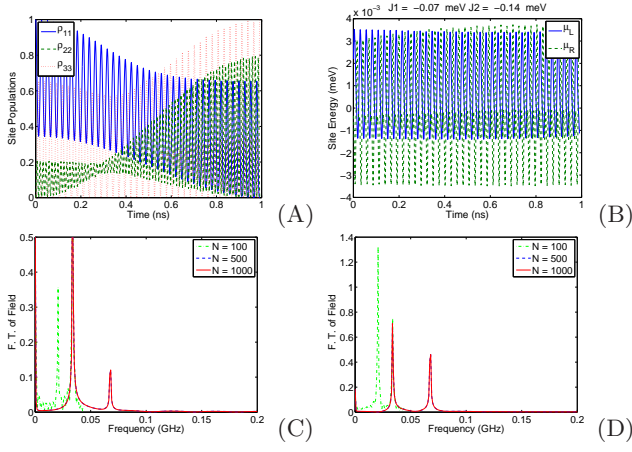


FIG. 1: (color online) Time dependence of site populations for electron shuttling across a triple quantum dot when acted on by time dependent voltages optimized to achieve minimal heating (i.e., minimal pulse energy). (A) Quantum dot populations for sites 1, 2, and 3, as a function of time. Blue solid line:  $\rho_{11}$ ; Green dashed line:  $\rho_{22}$ ; Red dotted line:  $\rho_{33}$ .  $J_1$  and  $J_2$  were set to  $-0.07$  and  $-0.14$  meV, respectively. (B) Optimal control voltages. Blue solid:  $\mu_L$ ; Green dashed:  $\mu_R$ . The pulses were determined here for  $N = 1000$  segments. (C) and (D) The Fourier transform of  $\mu_L$  and  $\mu_R$ , respectively, at different numbers of segments. We note that the form of the pulses converge at  $N = 500$ , after which pulses and site populations are indistinguishable from the corresponding values obtained with  $N = 1000$ .

The dynamics of the momentum functions  $\phi$  are obtained from Eq. (19) as

$$\begin{aligned}
 \dot{\phi}_1 &= J_2\phi_3 - \phi_4\phi_7/2 - \sqrt{3}/6\phi_4\phi_8 \\
 \dot{\phi}_2 &= -J_1\phi_3 - \phi_5\phi_8/\sqrt{3} \\
 \dot{\phi}_3 &= -J_2\phi_1 + J_1\phi_2 + \phi_6\phi_7/2 + \sqrt{3}/2\phi_6\phi_8 \\
 \dot{\phi}_4 &= \phi_1\phi_7/2 + \sqrt{3}/6\phi_1\phi_8 - J_2\phi_6 - 2J_1\phi_7 \\
 \dot{\phi}_5 &= \phi_2\phi_8/\sqrt{3} + J_1\phi_6 + J_2\phi_7 - \sqrt{3}J_2\phi_8 \\
 \dot{\phi}_6 &= -\phi_3\phi_7/2 - \sqrt{3}/2\phi_3\phi_8 + J_2\phi_4 - J_1\phi_5 \\
 \dot{\phi}_7 &= 2J_1\phi_4 - J_2\phi_5 \\
 \dot{\phi}_8 &= \sqrt{3}J_2\phi_5.
 \end{aligned} \tag{26}$$

For the derivation of the gradient of the fidelity and an explicit expression for this system, see Appendices A and B.

The optimized pulses for transfer with  $J_1$  set to  $-0.07$  meV and  $J_2$  set to  $-0.14$  meV are given in Fig. 1. The transfer time was taken to be 1 ns. The algorithm converges at  $N = 500$  slices of the time interval. The correlation between neighboring time steps can be seen as the optimized pulses are dominated by a small number of frequency components.

## V. IONIZED DONOR CHAIN

In this section we apply our control algorithm to the ionized donor chain studied in Ref. [5]. The system consists of three singly ionized phosphorus donors in silicon, and one electron shared in the system. The electron begins on the first phosphorus, site 1, and the pulses are designed to move this electron to site 3. The Hamiltonian is given by:

$$H = \begin{bmatrix} 0 & -\Omega_{12}(t) & 0 \\ -\Omega_{12}(t) & \Delta & -\Omega_{23}(t) \\ 0 & -\Omega_{23}(t) & 0 \end{bmatrix}. \tag{27}$$

Here the control terms are  $\Omega_{12}$  and  $\Omega_{23}$ , which are the coherent tunneling rate between adjacent dopants. Under the basis in Eq. (4), this Hamiltonian can be written as

$$iH = -\Omega_{12}X_1 - \Omega_{23}X_2 - \frac{\Delta}{2}X_7 + \frac{\Delta}{2\sqrt{3}}X_8 + \frac{\Delta}{3}iI_3. \tag{28}$$

We can drop the term  $\frac{\Delta}{3}iI_3$  as it commutes with all the other terms and thus contributes only a global phase. Consider the following minimum energy cost function

$$\min \frac{1}{2} \int_0^T (\Omega_{12}^2(\tau) + \Omega_{23}^2(\tau)) d\tau$$

with the initial and terminal states given in Eqs. (5)-(6). Following the procedure in Sec. III, we find that the parameters in the Hamiltonian of Eq. (3) are

$$u_1 = -\Omega_{12}, \quad u_2 = -\Omega_{23}, \quad a_7 = -\frac{\Delta}{2}, \quad a_8 = \frac{\Delta}{2\sqrt{3}},$$

and the running cost is

$$L(u) = \frac{u_1^2}{2} + \frac{u_2^2}{2}.$$

The optimality condition (16) yields

$$\phi_1 = u_1, \quad \phi_2 = u_2,$$

and hence the optimal controls are given by

$$\Omega_{12} = -\phi_1, \quad \Omega_{23} = -\phi_2. \tag{29}$$

For the Hamiltonian of Eq. (28), the dynamics of  $\phi$  in Eq. (19) becomes

$$\dot{\phi}_l = \sum_{i=1}^8 \left( \phi_1 C_{1l}^i + \phi_2 C_{2l}^i - \frac{\Delta}{2} C_{7l}^i + \frac{\Delta}{2\sqrt{3}} C_{8l}^i \right) \phi_i, \tag{30}$$

Substituting the values of structure constants  $C_{ij}^k$  in Eq. (22) into Eq. (30) yields the complete dynamics of  $\phi$ :

$$\begin{aligned}
\dot{\phi}_1 &= \phi_2\phi_3 + \Delta\phi_4 \\
\dot{\phi}_2 &= -\phi_1\phi_3 - \Delta\phi_5 \\
\dot{\phi}_3 &= 0 \\
\dot{\phi}_4 &= -\Delta\phi_1 - \phi_2\phi_6 - 2\phi_1\phi_7 \\
\dot{\phi}_5 &= \Delta\phi_2 + \phi_1\phi_6 + \phi_2\phi_7 - \sqrt{3}\phi_2\phi_8 \\
\dot{\phi}_6 &= \phi_2\phi_4 - \phi_1\phi_5 \\
\dot{\phi}_7 &= 2\phi_1\phi_4 - \phi_2\phi_5 \\
\dot{\phi}_8 &= \sqrt{3}\phi_2\phi_5.
\end{aligned} \tag{31}$$

The required matrices for the gradient algorithm for this systems are given in Appendix C.

In Fig. 2, the optimized pulses are shown for  $\Delta = 2.7$  meV and a transfer time of 1 ns. This choice of parameters is consistent with the values calculated using tight binding theory [7]. In Fig. 2(A), the populations of each site are shown as a function of time, the population is fully transferred from the first to the third site. The maximum magnitude of the pulses is on the order of magnitude of  $10^{-4}$  meV. Using the guideline for adiabatic transfer in Ref. [5],  $3.75 \approx \Omega_{max}t_{max}/\pi$ , this pulse magnitude would require a transfer time of 2.5 ns, or conversely the transfer time of 1 ns would require a pulse 2.5 times larger.

Since one of the main qubits of interest for solid-state quantum logic is phosphorus-doped silicon, where quantum information may be stored in either or both the spin of the electrons and nuclei [1–3] we have also investigated the performance of these optimal shuttling pulses in transmitting a hybrid electron-nuclear hyperfine spin state together with the spatial transfer of the electron. Here we assess the robustness of this procedure with respect to the spin states.

The hyperfine interaction was modeled as an on-site interaction of the electron spin ( $\sigma_e$ ) with the spin of the nucleus at each site  $i$  ( $\sigma_{N_i}$ ). To this we add the Zeeman interaction of each spin with the magnetic field  $B$ , to obtain the spin Hamiltonian

$$H_{spin} = B\gamma_e\sigma_e^z + \sum_i A\sigma_e \cdot \sigma_{N_i}|i\rangle\langle i| - B\gamma_N\sigma_{N_i}^z, \tag{32}$$

where  $A$  is the hyperfine constant and  $\gamma_e$  and  $\gamma_N$  are the electron and nuclear gyromagnetic ratios. Note that we have chosen the sign convention in which  $\gamma_e$  is positive. The eigenstates of the spin Hamiltonian (Eq. (32)) can be used to store quantum information. These states consist of the electron-nuclear spin aligned states  $|\uparrow\uparrow\rangle$  and  $|\downarrow\downarrow\rangle$ , and linear combinations of the anti-aligned states  $|\uparrow\downarrow\rangle$  and  $|\downarrow\uparrow\rangle$ , where the double arrows represent the electron spin and the single arrows represent the nuclear spin. As the magnetic field is increased, the eigenstates are dominated by one of the anti-aligned states, and at zero magnetic field the eigenstates are an equal superposition.

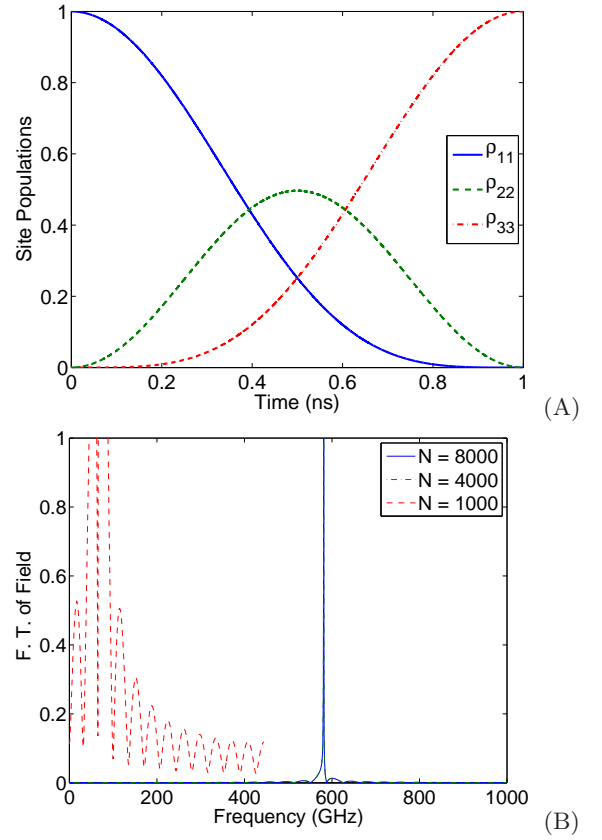


FIG. 2: (color online) Time dependence of site populations for electron shuttling across a chain of three singly ionized phosphorus ions, when acted on by time dependent voltages optimized to achieve minimal heating (i.e., minimal pulse energy). (A) Electron populations on donor sites 1, 2, and 3, as a function of time. Blue solid:  $\rho_{11}$ ; Green dashed:  $\rho_{22}$ ; Red dash-dot:  $\rho_{33}$ . The value of  $\Delta$  was set to 2.7 meV. (B) Fourier transform of the optimal control pulse  $\Omega_{12}$ . The second control pulse  $\Omega_{23}$  has the same frequency components as  $\Omega_{12}$  with a phase difference of  $-1.719$  rad. The time-domain pulses oscillate with a very high frequency, corresponding to the 2.7 meV value of  $\Delta$ , and so are not shown here. The optimal pulses are found converge at  $N = 8000$  segments.

Combined with the spatial Hamiltonian of Eq. (27), the entire Hamiltonian then given by

$$\begin{aligned}
H &= -\Omega_{12}(t) (|1\rangle\langle 2| + |2\rangle\langle 1|) \\
&\quad -\Omega_{23}(t) (|2\rangle\langle 3| + |3\rangle\langle 2|) \\
&\quad + \Delta|2\rangle\langle 2| + B\gamma_e\sigma_e^z - B\gamma_N (\sigma_{N_1}^z + \sigma_{N_2}^z + \sigma_{N_3}^z) \\
&\quad + A (\sigma_e|1\rangle\langle 1| \cdot \sigma_{N_1} + \sigma_e|2\rangle\langle 2| \cdot \sigma_{N_2} + \sigma_e|3\rangle\langle 3| \cdot \sigma_{N_3}).
\end{aligned} \tag{33}$$

For the phosphorus donor system, a hyperfine interaction with a splitting of  $A = 117.5$  MHz was used [41]. Results are shown in Fig. 3 for no external magnetic field (A) and for a field of 500 G (B). The spins of the nuclei at sites 2 and 3 are initialized into the  $\uparrow$  state, while on site 1 the electron-nuclear system is initialized into one of four hyperfine eigenstates (each panel of Fig. 3 rep-

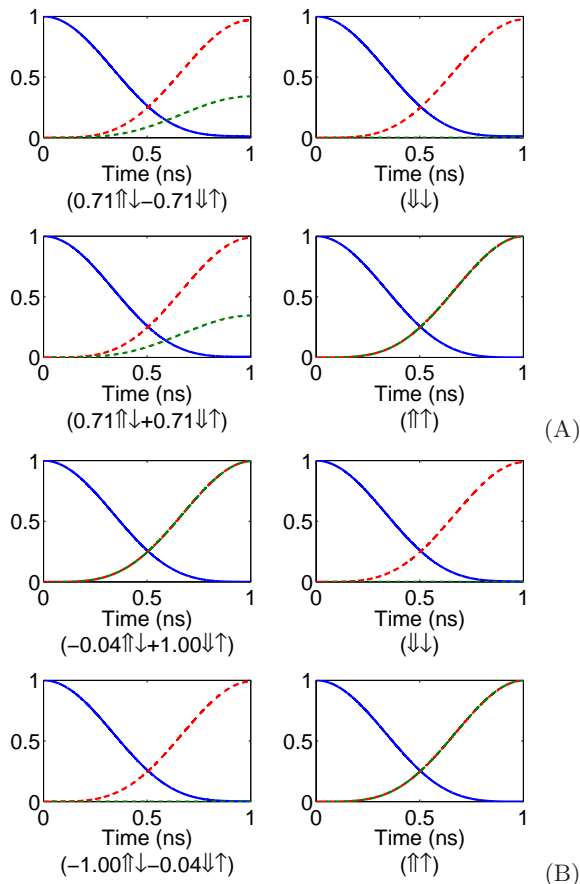


FIG. 3: (color online) (A) Time dependence of site populations on for electron shuttling across a chain of three single ionized phosphorus atoms when the spatial shuttling Hamiltonian is supplemented by the spin Hamiltonian, (32) at zero magnetic field. We show the transfer of all four hyperfine eigenstates accessible to the electron on site 1, under the pulses optimized solely for spatial shuttling in Fig. 2. The solid blue and dashed red lines show the population on sites 1 and 3, respectively, as before. The dashed green line shows measure  $D$  (Eq. (34)) of the hyperfine state transfer at site 3. (B) Same as (A), but in the presence of a finite magnetic field (500 G). The figures show that hyperfine states which align the nuclear spin with the magnetic field can be robustly transferred, independent of the magnetic field value, while transfer of the spin flipped states is energetically forbidden. See text for detailed explanation.

resents starting in a different hyperfine eigenstate; the coefficients of each eigenstate are shown under the figure). The distance measure ( $D$ ) shown in Fig. 3 is a measure of the fidelity of transfer of this hyperfine state,

$$D = 1 - \|\rho_T - \rho_{hf}\|_2. \quad (34)$$

Here  $\rho_{hf}$  is the density matrix for one of the hyperfine pure states (the spin-aligned states or the anti-aligned linear combinations), and  $\rho_T$  is the reduced density matrix of the site 3 nuclear and electron spin at the end of the spatial transfer. The norm used in Eq. (34) is

the induced 2-norm of the difference matrix, also known as the spectral norm, which is the maximum singular value of the matrix [42]. We have also calculated the fidelity [43, 44], the trace distance [43], and the Frobenius norm of the difference matrix [42]. While all norms show a similar picture regarding which states are transferred, the measure  $D$  has the pictorial advantage of following the population on the third site when full transfer is occurring, as well as remaining zero when the fidelity is zero, unlike the Frobenius norm.

At all magnetic fields, the  $|\uparrow\uparrow\rangle$  state can be transferred completely from site 1 to site 3, because with all of the nuclear spins up the electrons remain in the hyperfine eigenstate, no matter which spatial site it is on. Conversely, the hyperfine state  $|\downarrow\downarrow\rangle$  cannot be transferred at any magnetic field value, because transfer of this spin state requires flipping the spins of the nuclei on sites 2 and 3, which is not allowed energetically. The corresponding spatial fidelities of the state transfer are given in Table I for all possible initial spin eigenstates. It is evident that the transfer fidelity for the spatial degrees of freedom are only slightly affected by the spin interactions. Additional calculations have shown that for larger hyperfine constants the spatial transfer of the electron can be reduced significantly in the presence of the hyperfine interaction. For the linear combinations of spin states,  $|\uparrow\downarrow\rangle$  and  $|\downarrow\uparrow\rangle$ , partial spin transfers can be accomplished corresponding to the contribution from the component which has the nuclear spin up. This can be understood because as the magnetic field is turned on (Fig. 3(B)) and the relative magnitude of the two components in the linear combination becomes asymmetric, the transfer of the component which becomes primarily nuclear spin up can be achieved while transferring the component which becomes primarily nuclear spin down cannot. It should be noted that even in the case of a 500 G magnetic field, two hyperfine states can nevertheless be transferred spatially with high fidelity, suggesting their potential use as a mobile qubit.

TABLE I: The spatial fidelity for transfer starting from the left dopant in a given hyperfine eigenstate. The first and third columns give the eigenstate at  $B = 0G$  and  $B = 500G$ , respectively. The second and fourth columns give the corresponding spatial fidelity.

	$B = 0G$	$B = 500G$	
$0.71 \uparrow\downarrow - 0.71 \downarrow\uparrow$	0.9691	$-0.04 \uparrow\downarrow + 1.00 \downarrow\uparrow$	0.9970
$\downarrow\downarrow$	0.9740	$\downarrow\downarrow$	0.9873
$0.71 \uparrow\downarrow + 0.71 \downarrow\uparrow$	0.9870	$-1.00 \uparrow\downarrow - 0.04 \downarrow\uparrow$	0.9913
$\uparrow\uparrow$	1.00	$\uparrow\uparrow$	1.00

## VI. CONCLUSION

In this paper we have formulated the general problem of solid-state electron shuttling as a state transfer prob-



lem in optimal control theory. We derived the underlying dynamical equations that govern the time evolution of optimal control fields. Use of a momentum function was shown to lead to an effective algorithm with a small number of optimizing variables that requires numerical solution of an initial value problem rather than a two-point boundary problem. We demonstrated the efficacy of our algorithm with application to two physical examples.

First, we determined the control pulses for state transfer between left and right quantum dots in a triple quantum dot system. Since hyperfine interactions in lateral quantum dots can be small, such spatial transfer allows the ability to transmit quantum information and possibly use this ability to couple qubits. Second, we applied the optimal control approach to the system of shuttling of an electron along an ionized phosphorus donor chain in silicon. We again determined optimal control pulses for spatial transfer, finding a significant reduction in time and energy of the optimal pulses compared to those required by adiabatic protocols. For the shuttling across donor chains we also expanded the Hamiltonian to include magnetic interactions of the electron spin with the donor nuclear spins and of both electron and nuclear spins with external magnetic fields and then investigated the robustness of transfer of the hyperfine spin state states under these optimal pulses to variations in the magnetic field strength. For a magnetic field strength of 500 G (0.05 T), we find that two hyperfine states of the electron-nucleus on a given donor can be transferred across the chain to a distant donor with high fidelity. As the external field is decreased to zero, however, only one of four hyperfine states can be spatially transferred with high fidelity. Therefore, in order to transfer spin quantum information in a donor chain within a low-field environment, it will be necessary to design control pulses which are optimized for both spin and spatial dynamics. This will be addressed in a future publication.

### Acknowledgments

JZ thanks the financial support from the Innovation Program of Shanghai Municipal Education Commission under Grant No. 11ZZ20, Shanghai Pujiang Program under Grant No. 11PJ1405800, NSFC under Grant No. 61174086, Project-sponsored by SRF for ROCS SEM, State Key Laboratory of Precision Spectroscopy (ECNU), and State Key Lab of Advanced Optical Communication Systems and Networks (SJTU), China. LG and KBW thank NSA (Grant No. MOD713106A) for financial support. XD thanks the University of California-Berkeley College of Chemistry for a Summer Research Stipend.

### Appendix A: Derivation of $\frac{dF}{d\phi_l(0)}$

In this appendix, we derive the gradient of the fidelity  $F$  with respect to  $\phi(0)$ . This gradient of performance with respect to initial conditions of the momentum functions is required for step 4 of the gradient algorithm and is the key component of the algorithm to find the optimal control fields  $u_l(t)$ . By the chain rule, we have

$$\begin{aligned} \frac{dF}{d\phi_l(0)} &= \sum_{k=0}^{N-1} \sum_{m \in \overline{M}} \frac{dF}{du_m(k)} \frac{du_m(k)}{d\phi_l(0)} \\ &= \sum_{k=0}^{N-1} \sum_{m=1}^p \sum_{s=1}^8 \frac{dF}{du_m(k)} \frac{du_m(k)}{d\phi_s(k)} \frac{d\phi_s(k)}{d\phi_l(0)}, \end{aligned} \quad (\text{A1})$$

where  $\overline{M}$  is an index set of all the control fields. We thus need to derive the three differentials in each term on the right hand side of Eq. (A1).

1. We first consider the second term,  $\frac{du_m(k)}{d\phi_s(k)}$ . From Eq. (16), we obtain

$$\frac{d}{d\phi_s} \left( \frac{dL}{du_m} \right) = \frac{d}{d\phi_s} \phi_m = \delta_{ms}. \quad (\text{A2})$$

Because the running cost  $L$  is defined as a function of only the control fields  $u$  as in Eq. (7),  $\frac{dL}{du_m}$  is also a function of  $u$  only. Therefore, we can obtain  $\frac{du_m(k)}{d\phi_s(k)}$  by solving the algebraic equation Eq. (A2). For example, when  $L$  is taken as a quadratic function  $L = \frac{1}{2}(u_1^2 + u_2^2)$ , it is straightforward to show that  $\frac{du_m}{d\phi_s} = \delta_{ms}$ .

2. Next we consider the third term,  $\frac{d\phi_s(k)}{d\phi_l(0)}$ , *i.e.* the derivative of the momentum functions with respect to their initial conditions. These derivations may be obtained from Eq. (19). We rewrite Eq. (19) as a vector differential equation

$$\dot{\phi} = S(\phi), \quad (\text{A3})$$

with  $\phi = [\phi_1 \ \dots \ \phi_8]$  and where we have used the relation between the control functions  $u$  and the momentum functions  $\phi$  given by Eq. (16) to write the right hand side as a function of  $\phi$  alone, *i.e.*  $S(\phi)$ . Note that the form of  $S(\phi)$  will depend on the form of the cost function  $L$ . Differentiating both sides of Eq. (A3) with respect to  $\phi(0)$ , we now obtain

$$\frac{d}{d\phi(0)} \dot{\phi} = \frac{d}{d\phi(0)} S(\phi) = DS(\phi) \frac{d\phi}{d\phi(0)}, \quad (\text{A4})$$

where the Jacobian matrix  $DS(\phi)$  is given by

$$DS(\phi) = \begin{bmatrix} \frac{\partial S_1}{\partial \phi_1} & \dots & \frac{\partial S_1}{\partial \phi_8} \\ \vdots & & \vdots \\ \frac{\partial S_8}{\partial \phi_1} & \dots & \frac{\partial S_8}{\partial \phi_8} \end{bmatrix}, \quad (\text{A5})$$

and

$$\frac{d\phi}{d\phi(0)} = \begin{bmatrix} \frac{\partial\phi_1}{\partial\phi_1(0)} & \cdots & \frac{\partial\phi_1}{\partial\phi_s(0)} \\ \vdots & & \vdots \\ \frac{\partial\phi_s}{\partial\phi_1(0)} & \cdots & \frac{\partial\phi_s}{\partial\phi_s(0)} \end{bmatrix}. \quad (\text{A6})$$

From Proposition 6.1 of Chapter 1 in Ref. [45], we have

$$\frac{d}{d\phi(0)} \dot{\phi} = \frac{d}{dt} \frac{d\phi}{d\phi(0)}, \quad (\text{A7})$$

that is, it is legitimate to change the order of the differentials with respect to  $t$  and  $\phi(0)$ . Combining Eq. (A4) and Eq. (A7), we then arrive at the following differential equation that is satisfied by  $\frac{d\phi}{d\phi(0)}$ :

$$\frac{d}{dt} \frac{d\phi}{d\phi(0)} = DS(\phi) \frac{d\phi}{d\phi(0)}, \quad (\text{A8})$$

with initial condition

$$\left. \frac{d\phi}{d\phi(0)} \right|_{t=0} = I. \quad (\text{A9})$$

Solving this differential equation Eq. (A8), with initial condition Eq. (A9), yields the desired derivatives  $\frac{d\phi_s(k)}{d\phi_i(0)}$ .

3. Lastly we derive an explicit form for  $\frac{dF}{du_m(k)}$ , the desired performance gradient with respect to the physical control fields. From Eq. (3), we have

$$iH(k) = \sum_{l=1}^8 a_l X_l + \sum_{l=1}^8 u_l(k) X_l, \quad (\text{A10})$$

and  $U_k = e^{-iH(k)\Delta t}$ , where  $k = 0, \dots, N-1$ . Define

$$\begin{aligned} \rho_k &= U_{k-1} \cdots U_0 \rho_0 U_0^\dagger \cdots U_{k-1}^\dagger, \\ \Lambda_k &= U_k^\dagger \cdots U_{N-1}^\dagger \rho_T U_{N-1} \cdots U_k. \end{aligned}$$

Then  $\rho_N = \rho(T)$ ,  $\Lambda_N = \rho_T$ , and

$$\begin{aligned} F &= \text{Tr} \rho_T \rho(T) = \text{Tr} \Lambda_N \rho_N = \text{Tr} \Lambda_{N-1} \rho_{N-1} \\ &= \cdots = \text{Tr} \Lambda_1 \rho_1 = \text{Tr} \Lambda_0 \rho_0. \end{aligned} \quad (\text{A11})$$

It follows that

$$\begin{aligned} \frac{dF}{du_m(k)} &= \frac{d \text{Tr} \Lambda_{k+1} \rho_{k+1}}{du_m(k)} = \frac{d \text{Tr} \Lambda_{k+1} U_k \rho_k U_k^\dagger}{du_m(k)} \\ &= \text{Tr} \Lambda_{k+1} \left( \frac{dU_k}{du_m(k)} \rho_k U_k^\dagger + U_k \rho_k \frac{dU_k^\dagger}{du_m(k)} \right). \end{aligned} \quad (\text{A12})$$

From the following formula [46]

$$\left. \frac{d}{dv} e^{-i(H_a + vH_b)t} \right|_{v=0} = -i \int_0^t e^{-iH_a\tau} H_b e^{iH_a\tau} d\tau e^{-iH_a t}, \quad (\text{A13})$$

we have

$$\frac{dU_k}{du_m(k)} = - \int_0^{\Delta t} e^{-iH(k)\tau} X_m e^{iH(k)\tau} d\tau U_k. \quad (\text{A14})$$

Substituting Eq. (A14) into (A12), we obtain

$$\begin{aligned} \frac{dF}{du_m(k)} &= \text{Tr} \Lambda_{k+1} \left( - \int_0^{\Delta t} e^{-iH(k)\tau} X_m e^{iH(k)\tau} d\tau \rho_{k+1} \right. \\ &\quad \left. + \rho_{k+1} \int_0^{\Delta t} e^{-iH(k)\tau} X_m e^{iH(k)\tau} d\tau \right) \\ &= \text{Tr} [\Lambda_{k+1}, \rho_{k+1}] \int_0^{\Delta t} e^{-iH(k)\tau} X_m e^{iH(k)\tau} d\tau. \end{aligned}$$

Since  $H(k)$  is a Hermitian matrix, we can diagonalize it as

$$H(k) = T(k) \Gamma(k) T^\dagger(k), \quad (\text{A15})$$

where  $T(k)$  is a unitary matrix and  $\Gamma(k) = \text{diag}\{\gamma_1, \gamma_2, \gamma_3\}$ . Therefore,

$$\begin{aligned} &\int_0^{\Delta t} e^{-iH(k)\tau} X_m e^{iH(k)\tau} d\tau \\ &= \int_0^{\Delta t} T(k) e^{-i\Gamma(k)\tau} T^\dagger(k) X_m T(k) e^{i\Gamma(k)\tau} T^\dagger(k) d\tau \\ &= T(k) \int_0^{\Delta t} (T^\dagger(k) X_m T(k)) \odot \Theta d\tau T^\dagger(k), \end{aligned} \quad (\text{A16})$$

where  $\odot$  denotes the Hadamard product, *i.e.*, element-wise product, of two matrices, and  $\Theta_{ab} = e^{i(\gamma_b - \gamma_a)\tau}$ . For  $\gamma_a \neq \gamma_b$ , we define

$$\Phi_{ab} = \int_0^{\Delta t} \Theta_{ab} d\tau = \frac{e^{i(\gamma_b - \gamma_a)\Delta t} - 1}{i(\gamma_b - \gamma_a)};$$

and for  $\gamma_a = \gamma_b$ ,  $\Phi_{ab} = \Delta t$ . Therefore,

$$\begin{aligned} &\int_0^{\Delta t} e^{-iH(k)\tau} X_m e^{iH(k)\tau} d\tau \\ &= T(k) ((T^\dagger(k) X_m T(k)) \odot \Phi) T^\dagger(k), \end{aligned}$$

and

$$\begin{aligned} \frac{dF}{du_m(k)} &= \text{Tr} ([\Lambda_{k+1}, \rho_{k+1}] T(k) \\ &\quad \cdot ((T^\dagger(k) X_m T(k)) \odot \Phi) T^\dagger(k)). \end{aligned} \quad (\text{A17})$$

We now have all the three factors in each term in the sum for the desired performance gradient with respect to initial conditions,  $\frac{dF}{d\phi_i(0)}$ , Eq. (A1).

## Appendix B: Form of $\frac{dF}{d\phi_i(0)}$ for electron shuttling across triple quantum dot

Now for the triple quantum dot system in Section IV, the gradient of the fidelity  $F$  with respect to  $\phi_i(0)$  is then

derived as

$$\begin{aligned} \frac{dF}{d\phi_l(0)} &= \sum_{k=0}^{N-1} \sum_{m \in \{7,8\}} \sum_{s=1}^8 \frac{dF}{du_m(k)} \frac{du_m(k)}{d\phi_s(k)} \frac{d\phi_s(k)}{d\phi_l(0)}. \\ &= \sum_{k=0}^{N-1} \left( \frac{1}{4} \frac{dF}{du_7(k)} \frac{d\phi_7(k)}{d\phi_l(0)} + \frac{1}{4\sqrt{3}} \frac{dF}{du_7(k)} \frac{d\phi_8(k)}{d\phi_l(0)} \right. \\ &\quad \left. + \frac{1}{4\sqrt{3}} \frac{dF}{du_8(k)} \frac{d\phi_7(k)}{d\phi_l(0)} + \frac{5}{12} \frac{dF}{du_8(k)} \frac{d\phi_8(k)}{d\phi_l(0)} \right). \end{aligned}$$

The Jacobian matrix  $DS(\phi)$  (see Eq. (A5) for definition) is given in this case by

$$\begin{bmatrix} 0 & 0 & J_2 & -\frac{\phi_7}{2} & 0 & 0 & -\frac{\phi_4}{2} & -\frac{\sqrt{3}\phi_4}{6} \\ 0 & 0 & -J_1 & 0 & -\frac{\phi_8}{\sqrt{3}} & 0 & 0 & -\frac{\phi_5}{\sqrt{3}} \\ -J_2 & J_1 & 0 & 0 & 0 & \frac{\sqrt{3}\phi_8}{2} & \frac{\phi_6}{2} & \frac{\sqrt{3}\phi_6}{2} \\ \frac{\sqrt{3}\phi_8}{6} & 0 & 0 & 0 & 0 & -J_2 & \frac{\phi_1}{2} & \frac{\sqrt{3}\phi_1}{6} \\ +\frac{\phi_7}{2} & 0 & 0 & 0 & 0 & -2J_1 & -\frac{\phi_2}{\sqrt{3}} & -\frac{\phi_3}{\sqrt{3}} \\ 0 & \frac{\phi_8}{\sqrt{3}} & 0 & 0 & 0 & J_1 & J_2 & -\frac{\phi_2}{\sqrt{3}} \\ 0 & 0 & -\frac{\sqrt{3}\phi_8}{2} & J_2 & -J_1 & 0 & -\frac{\phi_3}{2} & -\frac{\sqrt{3}\phi_3}{2} \\ 0 & 0 & 0 & 2J_1 & -J_2 & 0 & 0 & 0 \\ 0 & 0 & 0 & 0 & \sqrt{3}J_2 & 0 & 0 & 0 \end{bmatrix}.$$

### Appendix C: Form of $\frac{dF}{d\phi_l(0)}$ for electron shuttling across ionized donor chain

For the ionized donor chain of Section V, the gradient of the fidelity  $F$  with respect to  $\phi_l(0)$  can then be derived

as

$$\frac{dF}{d\phi_l(0)} = \sum_{k=0}^{N-1} \left( \frac{dF}{du_1(k)} \frac{d\phi_1(k)}{d\phi_l(0)} + \frac{dF}{du_2(k)} \frac{d\phi_2(k)}{d\phi_l(0)} \right), \quad (\text{C1})$$

and the Jacobian matrix  $DS(\phi)$  is derived from Eq. (31) as

$$\begin{bmatrix} 0 & \phi_3 & \phi_2 & \Delta & 0 & 0 & 0 & 0 \\ -\phi_3 & 0 & -\phi_1 & 0 & -\Delta & 0 & 0 & 0 \\ 0 & 0 & 0 & 0 & 0 & 0 & 0 & 0 \\ -\Delta & -\phi_6 & 0 & 0 & 0 & -\phi_2 & -2\phi_1 & 0 \\ \phi_6 & \Delta + \phi_7 & 0 & 0 & 0 & \phi_1 & \phi_2 & -\sqrt{3}\phi_2 \\ -\phi_5 & -\sqrt{3}\phi_8 & 0 & 0 & 0 & 0 & 0 & 0 \\ 2\phi_4 & \phi_4 & 0 & \phi_2 & -\phi_1 & 0 & 0 & 0 \\ 0 & -\phi_5 & 0 & 2\phi_1 & -\phi_2 & 0 & 0 & 0 \\ 0 & \sqrt{3}\phi_5 & 0 & 0 & \sqrt{3}\phi_2 & 0 & 0 & 0 \end{bmatrix}.$$

For the particular Hamiltonian given in Eq. (28), we can derive an analytic solution for the decomposition in Eq. (A15). The corresponding eigenvalues of  $H(k)$  are

$$\gamma_1 = -\frac{\Delta}{3}, \quad \gamma_2 = \frac{\Delta + 3g_1}{6}, \quad \gamma_3 = \frac{\Delta - 3g_1}{6},$$

and the unitary matrix  $T(k)$  is

$$\begin{bmatrix} -\Omega_{23}/g_2 & \Omega_{12}/\sqrt{g_1(g_1 + \Delta)/2} & \Omega_{12}/\sqrt{g_1(g_1 - \Delta)/2} \\ 0 & -\sqrt{(g_1 + \Delta)/(2g_1)} & \sqrt{(g_1 - \Delta)/(2g_1)} \\ \Omega_{12}/g_2 & \Omega_{23}/\sqrt{g_1(g_1 + \Delta)/2} & \Omega_{23}/\sqrt{g_1(g_1 - \Delta)/2} \end{bmatrix},$$

where  $g_1 = \sqrt{\Delta^2 + 4\Omega_{23}^2 + 4\Omega_{12}^2}$  and  $g_2 = \sqrt{\Omega_{23}^2 + \Omega_{12}^2}$ .

- 
- [1] J. J. L. Morton, D. R. McCamey, M. A. Eriksson, and S. A. Lyon, *Nature* **479**, 345 (2011).
- [2] A. J. Skinner, M. E. Davenport, and B. E. Kane, *Phys. Rev. Lett.* **90**, 087901 (2003).
- [3] B. E. Kane, *Nature* **393**, 133 (1998).
- [4] K. Bergmann, H. Theuer, and B. W. Shore, *Rev. Mod. Phys.* **70**, 1003 (1998).
- [5] A. D. Greentree, J. H. Cole, A. R. Hamilton, and L. C. L. Hollenberg, *Phys. Rev. B* **70**, 235317 (2004).
- [6] L. C. L. Hollenberg, A. D. Greentree, A. G. Fowler, and C. J. Wellard, *Phys. Rev. B* **74**, 045311 (2006).
- [7] R. Rahman, R. P. Muller, J. E. Levy, M. S. Carroll, G. Klimeck, A. D. Greentree, and L. C. L. Hollenberg, *Phys. Rev. B* **82**, 155315 (2010).
- [8] B. Chen, W. Fan, and Y. Xu, *Phys. Rev. A* **83**, 014301 (2011).
- [9] D. Loss and D. P. DiVincenzo, *Phys. Rev. A* **57**, 120 (1998).
- [10] L. Jacak, J. Karsnyj, D. Jacak, W. Salejda, and A. Mitus, *Act. Phys. Polon. A* **99**, 277 (2000).
- [11] D. Culcer, L. Cywiński, Q. Li, X. Hu, and S. D. Sarma, *Phys. Rev. B* **80**, 205302 (2009).
- [12] Y. Hada and M. Eto, *Jpn. J. of Appl. Phys.* **43**, 7329 (2004).
- [13] B. M. Maune, M. G. Borselli, B. Huang, T. D. Ladd, P. W. Deelman, K. S. Holabird, A. A. Kiselev, I. Alvarado-Rodriguez, R. S. Ross, A. E. Schmitz, et al., *Nature* **481**, 344 (2012).
- [14] J. R. Petta, A. C. Johnson, J. M. Taylor, E. A. Laird, A. Yacoby, M. D. Lukin, C. M. Marcus, M. P. Hanson, and A. C. Gossard, *Science* **309**, 2180 (2005), ISSN 1095-9203.
- [15] J. M. Taylor, H. A. Engel, W. Dur, A. Yacoby, C. M. Marcus, P. Zoller, and M. D. Lukin, *Nat. Phys.* **1**, 177 (2005), ISSN 1745-2473.
- [16] C. Brif, D. L. Hocker, K. W. Moore, M. D. Grace, K. C. Young, T.-S. Ho, and H. Rabitz (2011), *in prep.*
- [17] K. W. Moore Tibbetts, C. Brif, M. D. Grace, A. Donovan, D. L. Hocker, T.-S. Ho, R.-B. Wu, and H. Rabitz, *Phys. Rev. A* **86**, 062309 (2012).
- [18] S. Sastry, *Nonlinear Systems: Analysis, Stability and Control* (Springer-Verlag, 1999).
- [19] L. Pontryagin, V. Boltyanskii, R. Gamkrelidze, and E. Mischenko, *The mathematical theory of optimal processes* (Wiley, New York, 1962).
- [20] A. I. Konnov and V. A. Krotov, *Automation and Remote*

- Control (1999).
- [21] S. E. Sklarz and D. J. Tannor, Phys. Rev. A **66**, 053619 (2002).
- [22] J. P. Palao and R. Kosloff, Phys. Rev. A **68**, 062308 (2003).
- [23] D. M. Reich, M. Ndong, and C. P. Koch, J. Chem. Phys. **136**, 104103 (2012).
- [24] J. E. Marsden and T. S. Ratiu, *Introduction to mechanics and symmetry* (Springer-Verlag, New York, 1998).
- [25] H. Georgi, *Lie Algebras In Particle Physics* (Westview Press, 1999), 2nd ed.
- [26] V. Jurdjevic and H. J. Sussmann, Journal of Differential Equations **12**, 313 (1972).
- [27] R. W. Brockett, in *Geometric methods in system theory*, edited by D. Q. Mayne and R. W. Brockett (Dordrecht, The Netherlands, 1973), pp. 43–82.
- [28] T. J. Tarn, G. Huang, and J. W. Clark, Mathematical Modelling **1**, 109 (1980).
- [29] G. M. Huang, T. J. Tarn, and J. W. Clark, J. Math. Phys. **24**, 2608 (1983).
- [30] V. Jurdjevic, *Geometric control theory* (Cambridge university press, 1997).
- [31] K. W. Moore, C. Brif, M. D. Grace, A. Donovan, D. L. Hocker, T.-S. Ho, R. Wu, and H. Rabitz (2011), arXiv:1112.0333.
- [32] A. P. Peirce, M. A. Dahleh, and H. Rabitz, Phys. Rev. A **37**, 4950 (1988).
- [33] W. Zhu and H. Rabitz, J. Chem. Phys. **109**, 385 (1998).
- [34] Y. Maday and G. Turinici, J. Chem. Phys. **118**, 8191 (2003).
- [35] Y. Ohtsuki, W. Zhu, and H. Rabitz, J. Chem. Phys. **110**, 9825 (1999).
- [36] Y. Ohtsuki, G. Turinici, and H. Rabitz, J. Chem. Phys. **120**, 5509 (2004).
- [37] P. Doria, T. Calarco, and S. Montangero, Phys. Rev. Lett. **106**, 190501 (2011).
- [38] A. E. Bryson and Y. C. Ho, *Applied optimal control: optimization, estimation, and control* (Hemisphere Publishing Corporation, 1975).
- [39] P. S. Krishnaprasad, in *Notes for Workshop on Mechanics, Holonomy, and Control*, CDC (IEEE, 1993).
- [40] N. Khaneja, T. Reiss, C. Kehlet, T. Schulte-Herbrüggen, and S. J. Glaser, J. of Magnetic Resonance **172**, 296 (2005).
- [41] G. Feher, Phys. Rev. **114**, 1219 (1959).
- [42] F. M. Callier and C. A. Desoer, *Linear system theory* (Springer-Verlag, London, UK, 1991).
- [43] M. A. Nielsen and I. L. Chuang, *Quantum Computation and Quantum Information* (Cambridge University Press, Cambridge, UK, 2000).
- [44] C. A. Fuchs (1996), arXiv:9601020.
- [45] M. E. Taylor, *Partial Differential Equations: Basic Theory* (Springer, 1996).
- [46] I. Najfeld and T. F. Havel, Advances in Applied Mathematics **16**, 321 (1995).